IEEE Access
Multidisciplinary | Rapid Review | Open Access Journal

Received January 25, 2019, accepted February 15, 2019, date of publication February 25, 2019, date of current version March 13, 2019.

Digital Object Identifier 10.1109/ACCESS.2019.2901680

A Variety of Engine Faults Detection Based on Optimized Variational Mode Decomposition-Robust Independent Component Analysis and Fuzzy C-Mean Clustering

XIAOYANG BI[1,2,3,4], SHUQIAN CAO[1,3,4], AND DAMING ZHANG[2]

[1]Department of Mechanics, Tianjin University, Tianjin 300354, China
[2]Department of Industrial Technology, California State University, Fresno, CA 93740, USA
[3]Tianjin Key Laboratory of Nonlinear Dynamics and Control, Tianjin 300354, China
[4]National Demonstration Center for Experimental Mechanics Education, Tianjin University, Tianjin 300354, China

Corresponding author: Shuqian Cao (sqcao@tju.edu.cn)

This work was supported by the National Science and Technology Support Program of China under Grant 2015BAF07B04.

ABSTRACT As one kind of current main power sources, internal combustion engines require high-reliability to ensure mechanical systems working well in normal operation. This paper studies vibration signals in order to detect multiple types of faults by a single channel signal. First, for the decomposition level of variational mode decomposition (VMD) which needs to be chosen non-automatically, this paper analyzes the features of various faults and optimizes the iteration initial values of center frequency so as to reduce the adverse effect of inappropriate decomposition level. Moreover, considering that VMD cannot decompose different signal sources in the same frequency, robust independent component analysis (ICA) is an excellent method to overcome this challenge. Then, the fourth-order cumulant of restructured signals from VMD and robust ICA is taken as fault indexes. Finally, because of the high error rate of original fuzzy C-Mean clustering, Euclidean distance between test points and cluster center of fuel injection failure is taken as a fault detection threshold in order to achieve high-recognition rate. In conclusion, through optimizing several algorithms, the purpose of detecting multiple types of faults by single channel signal is achieved in the current research.

INDEX TERMS IC Engine, fault diagnosis, vibration, variational mode decomposition (VMD).

I. INTRODUCTION

IC engines are one kind of currently main power sources which have been widely used in transportation and electricity generation because of its high thermal efficiency and power performance. An IC engine is an important assembly component of mechanical system whose working conditions influence the safety and reliability of the whole system [1], [2]. It is necessary to develop an accurate and fast algorithm to detect engine faults.

At the present stage, there are several methods to detect engine faults such as vibration detection method, noise detection method, oil analysis method [3]–[5]. Among those, oil analysis method is used for analyzing the physical and chemical characteristics of particles in lubricating oil to determine working conditions [6]. However, this method cannot detect faults in real time. It can only be used to identify fault sources after failures. Noise detection method uses radiated noise to diagnose faults, which could possibly be used for faults detection online. But the disadvantage of this method is that noise signals are easily affected by uncontrollable factors [7]. Compared to these fault sources, the vibration signal of diesel engines contains a lot of information related to working status and fault characteristic. Extracting characteristic parameters from vibration signal should be able to effectively identify the working status and related faults of diesel engines.

As the structure of diesel engines is very complex and there are many different vibration sources, that means the original vibration signal has to be analyzed by accurate algorithms [8], [9]. In recent years, many algorithms have been used for vibration signal processing [10], Siano and D'Agostino [11] collected vibration signals and calculated knock characteristic frequencies using Short time Fourier Transform (STFT). Wang *et al.* [12] proposed an adaptive

The associate editor coordinating the review of this manuscript and approving it for publication was Youqing Wang.

threshold wavelet denoising method which was successfully applied to diagnose fuel injection fault. Bustos *et al.* [13] used Empirical Mode Decomposition (EMD) to analyze vibration signals for railway vehicle faults detection. However, all of those algorithms have their own disadvantages, such as that STFT can't balance the resolution between time domain and frequency domain. Although wavelet method can adjust the resolution of time domain and frequency domain, it is not an adaptive method. Beyond that, there are no accepted selection criteria for wavelet basis, which affects the accuracy of decomposition [14]. EMD is a relatively adaptive algorithm but works as a recursive decomposition method. Mode mixing often occurs because errors accumulated in the formation process of envelopes [14]. In addition, end effect, over/under envelope, and low accuracy for signals with close frequencies in EMD are still unresolved problems [15]. The Ensemble Empirical Mode Decomposition (EEMD) method proposed by Wu and Huang [16] can improve the disadvantage of EMD method, but EEMD's computational efficiency limited its application for online detection.

Variational Mode Decomposition (VMD) is a new algorithm proposed by Dragomiretskiy and Zosso [17], [18] in 2014. This method uses variational model to replace the recursive decomposition model. It avoided inherent defects of recursive decomposition and showed better robustness. And, it can successfully separate two harmonic signals with similar frequencies. Compared with EEMD, VMD has high computational efficiency.

Due to these advantages, VMD algorithm has been widely used in the field of fault diagnosis. For instance, VMD method optimized by particle swarm was used to rolling bearing fault diagnosis by Yi *et al.* [19]. VMD method optimized by Support Vector Machine (SVM) has been used for mechanical fault analysis [20]–[22]. Furthermore, VMD algorithm is also applied in the field of engine fault diagnosis [23], [24].

Independent Component Analysis (ICA) was originally developed for signal processing applications and later has been generalized for feature extraction. This method is a Blind Source Separation (BSS) approach [25]. Even though the transmission channel characteristics and signal sources are unknown, each signal source can be separated from it only by measuring the signal and using the ICA algorithm [26], [27].

Previous research results indicated that [28]–[30], there are two main challenges which need to be attained. One is improving the calculation efficiency of VMD and robust Independent Component Analysis (ICA) with high accuracy. Another is detecting several different faults by single channel signal. In the current study, the research process can be summarized as the following steps. Firstly, decomposing vibration signals by VMD. Secondly, analyzing the results by Robust ICA. Finally, the fourth-order cumulants of VMD and robust ICA decomposing restructure signals are taken as fault indices in order to detect faults by fuzzy C-mean clustering (FCM) and Euclidean distance.

This paper is organized as follows. The research background and significance are introduced in Section 1, and algorithms are introduced in Section 2. The experiment process is briefly described in Section 3. VMD is optimized in Section 4. The fault type distinction by optimized FCM is in Section 5, and finally conclusions and outlook are in Section 6.

II. ALGORITHM THEORIES

A. VMD ALGORITHM

1) THE VMD ALGORITHM THEORY

The purpose of VMD algorithm is to decompose input signal f into several Intrinsic Mode Functions (IMFs) u_k. The u_k compacts around a center pulsation and reconstructs original signal [17].

It is needed to estimate the bandwidth of u_k. Firstly, the unilateral spectrum of u_k is obtained by Hilbert transform:

$$\left[\delta(t)+\frac{j}{\pi t}\right]u_k(t) \tag{1}$$

Next, an estimated center frequency $e^{-j\omega_k t}$ is mixed into the analytic signal, so the spectrum of u_k will be modulated to baseband:

$$\left[\delta(t)+\frac{j}{\pi t}\right]u_k(t)*e^{-j\omega_k t} \tag{2}$$

The bandwidth of u_k can be obtained by computing its squared L2-norm. Constrained variational problem is as shown:

$$\begin{cases}\min\limits_{\{u_k\},\{w_k\}}\left\{\sum_k\left\|\partial_t\left[\delta(t)+\frac{j}{\pi t}\right]u_k(t)*e^{-j\omega_k t}\right\|_2^2\right\}\\ s.t\ \ \sum_k u_k=f\end{cases} \tag{3}$$

where $\{u_k\}=\{u_1,\cdots,u_k\}$ and $\{\omega_k\}=\{\omega_1,\cdots,\omega_k\}$ are the shorthand notations for the set of all modes and their center frequencies, $\sum k=\sum_{k=1}^{k}$ is the summation over all modes.

In order to solve the constrained variational problem, quadratic penalty term α and Lagrange multiplier λ are introduced. The augmented Lagrange L is as shown:

$$\begin{aligned}&L(\{u_k\},\{\omega_k\},\lambda)\\&=\alpha\sum_k\left\|\partial_t[(\delta(t)+\frac{j}{\pi t})*u_k(t)]e^{-j\omega_k t}\right\|_2^2\\&\quad+\left\|f(t)-\sum_k u_k(t)\right\|_2^2+\left\langle\lambda(t),f(t)-\sum_k u_k(t)\right\rangle\end{aligned} \tag{4}$$

The quadratic problem can be solved easily in Fourier domain [17]:

$$\hat{u}_k^{n+1}(\omega)=\frac{\hat{f}(\omega)-\sum i\neq k\hat{u}_i(\omega)+\frac{\hat{\lambda}(\omega)}{2}}{1+2\alpha(\omega-\omega_k)^2} \tag{5}$$

$$\omega_k^{n+1}=\frac{\int_0^\infty\omega\left|\hat{u}_k(\omega)\right|^2d\omega}{\int_0^\infty\left|\hat{u}_k(\omega)\right|^2d\omega} \tag{6}$$

The Lagrange multiplier λ is:

$$\hat{\lambda}^{n+1}(\omega)=\hat{\lambda}^n(\omega)+\tau(\hat{f}(\omega)-\sum_k\hat{u}_k^{n+1}) \tag{7}$$

The original minimization problem is founded as saddle point of augmented Lagrange. The Alternate Direction Method of Multipliers (ADMM) is used to update u_k, ω_k, λ. So the VMD algorithm is given in detail as follows:

1) The $\{u_k^1\}$, $\{\omega_k^1\}$, $\hat{\lambda}^1$ and n are initialized;
2) The u_k is updated by the formula (5);
3) The ω_k is updated by the formula (6);
4) The λ is updated by the formula (7);
5) The steps (2)-(7) are repeated until the iteration stop condition is met:

$$\sum_k (\left\| u_k^{n+!} - u_k^n \right\|_2^2 / \left\| u_k^n \right\|_2^2) < \varepsilon \tag{8}$$

As soon as the loop is completed, input signal will be decomposed into K modes.

2) ANALOG SIGNAL TEST

In order to confirm the advantage of VMD, an analog signal is decomposed by VMD and EMD. The analog signal is composed by several different frequency signals, as shown in Fig 1.

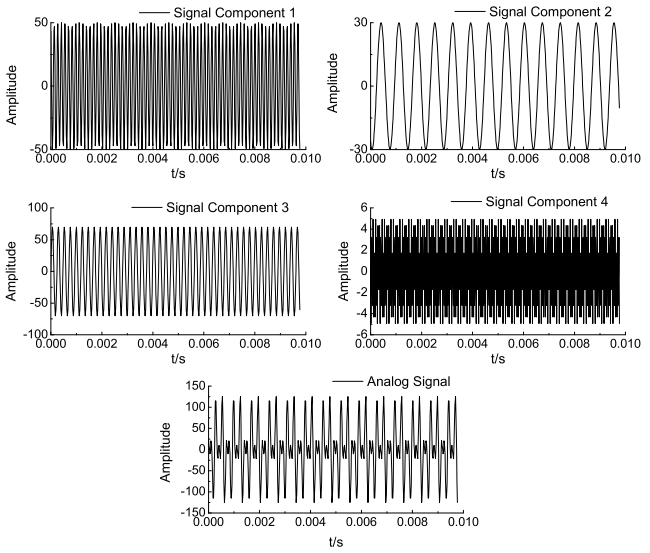

FIGURE 1. The analog signal.

Decomposing this analog signal by VMD, the number of modes is set as K = 4, as shown in Fig 2.

The result of EMD is obtained automatically by cut-off condition and only 4 of 7 modes are shown in Fig 3.

Fig 2 and Fig 3 showed that the result of VMD has obvious advantages. For example, it can decompose signals in close frequencies successfully. EMD not only can't do that, but also obtains result with end effect and illusive components. This demonstrate that introducing VMD into engine fault detection is feasible.

B. ICA ALGORITHM

VMD can be used for decomposing signals with different frequencies. Considering that engine vibration signals

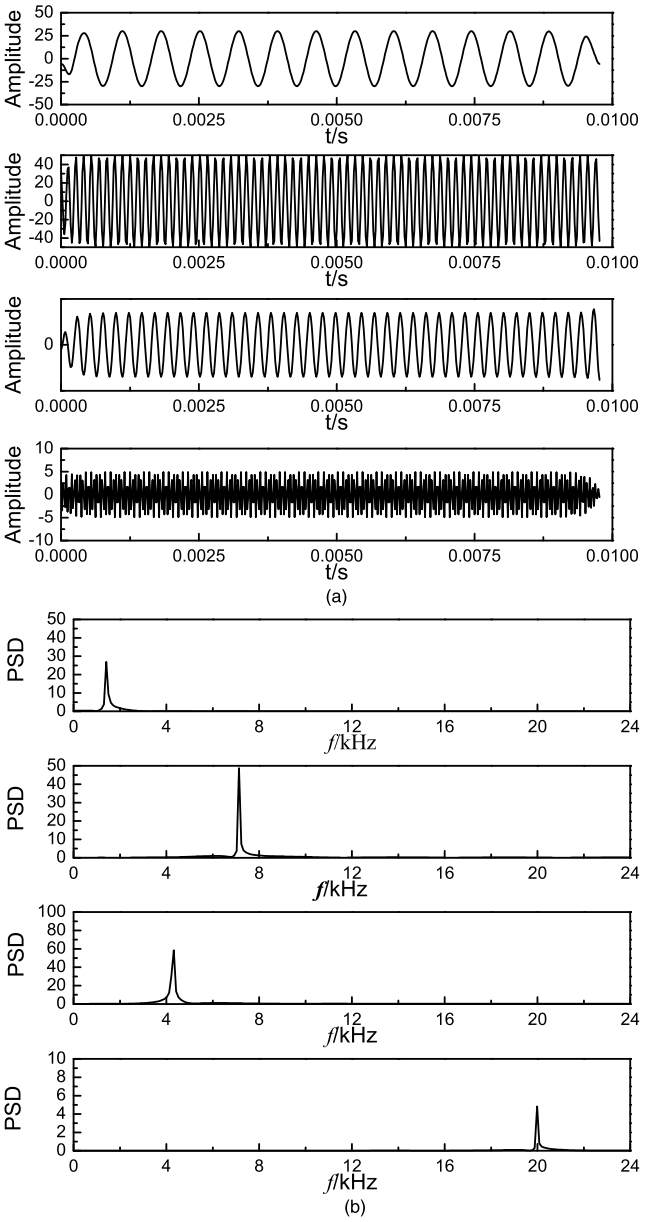

FIGURE 2. The results of VMD. (a) The time domain. (b) The frequency domain.

are complex, if they have vibration sources with the same frequency, it can be solved by ICA [31]–[33].

According to ICA, there are n independent signal sources and m sensors. Ignoring noise and transfer time in account, the signals received by sensors are linearly mixed source signals. They are:

$$X(t) = AS(t) \tag{9}$$

where $X(t) = [x_1(t), x_2(t), \cdots, x_m(t)]^T$ are measured signals, $S(t) = [s_1(t), s_2(t), \cdots, s_n(t)]^T$ are source signals, A is a m × n dimensional mixing matrix.

ICA aims to find a m × n dimensional separating matrix W with the unknown source signals S(t) and mixing matrix A.

$$W \approx A^{-1} \tag{10}$$

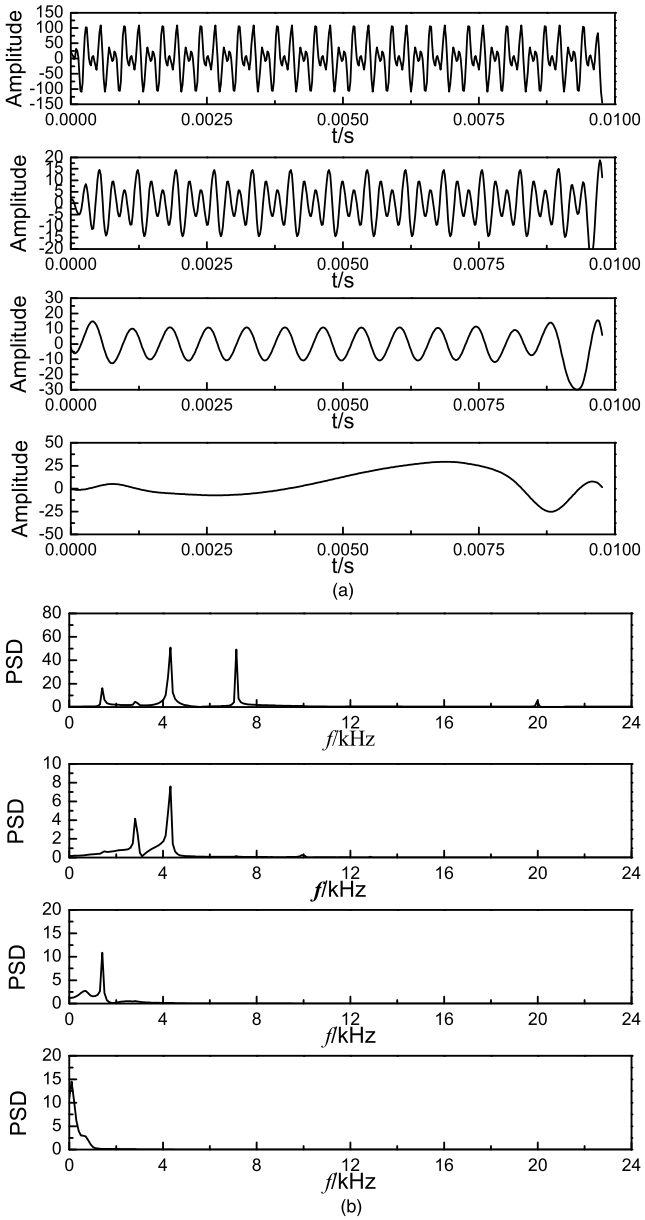

FIGURE 3. The results of EMD. (a) The time domain. (b) The frequency domain.

Substituting it to Formula (9) to get:

$$Y = WX = WAS = A^{-1}AS \tag{11}$$

The signal Y is considered as an approximate estimation of the source signal S(t).

C. FCM ALGORITHM

For the sake of detecting different types of faults, FCM is introduced and described as follows [34]:

There is set of sample data $X = \{x_1, x_2, \cdots, x_n,\}$ fuzzy membership matrix $U = [u_{ij}]_{c\times n}$ and cluster center $C = [c_1, c_2, \cdots, c_n]^T$. Where c is the number of cluster centers, n is the number of samples, u_{ij} is the membership of a point x_j to the cluster center c_j.

The Euclidean distance from x_j to c_j is:

$$d_{ij} = \|x_j - c_i\| = (x_j - c_i)^T(x_j - c_i) \tag{12}$$

The objective function of FCM is:

$$J(U, C) = \sum_{j=1}^{n}\sum_{i=1}^{n} u_{ij}^m d_{ij} \tag{13}$$

The objective function of FCM is minimized by means of iteration method as follows:

1) The number of cluster centers c, fuzzy weighted number m, iteration stop condition ε and maximum iterative number k_{max} are determined. The fuzzy membership matrix U is initialized;
2) The cluster centers are computed:

$$c_i = \sum_{j=1}^{n} u_{ij}^m x_j / \sum_{j=1}^{n} u_{ij}^m \tag{14}$$

3) The fuzzy membership matrix U is updated:

$$u_{ij} = 1/\sum_{k=1}^{c} (\frac{d_{ij}}{d_{kj}})^{2/(m-1)} \tag{15}$$

4) When $\|U^{k+1} - U^k\| \leq \varepsilon$ or the iterative number reaches k_{max}, stop the iteration.

D. HIGHER ORDER CUMULANT

Fourth order cumulant is one of higher order cumulants, whose principle is as follows [35]:

Supposing there is a random variable $x = [x_1, \cdots x_k]^T$, whose characteristic function is:

$$\Phi(\omega_1, \cdots \omega_k) = E\{exp[j(\omega_1 x_1 + \cdots + \omega_k x_k)]\} \tag{16}$$

Its $r = \nu_1 + \cdots \nu_k$ order partial derivative is:

$$\frac{\partial^{'}\Phi(\omega_1, \cdots \omega_k)}{\partial\omega_1^{\nu_1}\cdots\partial\omega_k^{\nu_k}} = j^r E\{x_1^{\nu_1}\cdots x_k^{\nu_k} e^{j(\omega_1 x_1 \cdots \omega_k x_k)}\} \tag{17}$$

If $\omega_1 = \cdots = \omega_k = 0$, the r-th order moment of x is:

$$\begin{aligned} m_{\nu_1\cdots\nu_k} &= E\{x_1^{\nu_1}\cdots x_k^{\nu_k}\} \\ &= (-j)^r \frac{\partial^r \Phi(\omega_1, \cdots \omega_k)}{\partial\omega_1^{\nu_1}\cdots\partial\omega_k^{\nu_k}} |\omega_1 = \cdots = \omega_k = 0 \end{aligned} \tag{18}$$

So, the r-th order cumulant of x is:

$$\begin{aligned} c_{\nu_1\cdots\nu_k} &= (-j)^r \frac{\partial^r \Psi(\omega_1, \cdots \omega_k)}{\partial\omega_1^{\nu_1}\cdots\partial\omega_k^{\nu_k}} |\omega_1 = \cdots = \omega_k = 0 \\ &= (-j)^r \frac{\partial^r ln\Phi(\omega_1, \cdots \omega_k)}{\partial\omega_1^{\nu_1}\cdots\partial\omega_k^{\nu_k}} |\omega_1 = \cdots = \omega_k = 0 \end{aligned} \tag{19}$$

The $\Phi_x(\omega_1 \cdots \omega_k)$ expanded by Taylor formula as shown below:

$$\begin{aligned} \Phi_x(\omega_1 \cdots \omega_k) \sum_{\nu_1+\cdots+\nu_k \leq n} &\frac{j^{\nu_1+\cdots+\nu_k}}{\nu_1!\cdots\nu_k!} \\ &\times m_{\nu_1,\cdots,\nu_k}\omega_1^{\nu_1}, \cdots \omega_k^{\nu_k} + o(|\omega|^n) \end{aligned} \tag{20}$$

So:

$$\begin{aligned} ln\Phi_x(\omega_1 \cdots \omega_k) = \sum_{\nu_1+\cdots+\nu_k \leq n} &\frac{j^{\nu_1+\cdots+\nu_k}}{\nu_1!\cdots\nu_k!} \\ &\times c_{\nu_1,\cdots,\nu_k}\omega_1^{\nu_1}, \cdots \omega_k^{\nu_k} + o(|\omega|^n) \end{aligned} \tag{21}$$

where $|\omega| = |\omega_1| + \cdots + |\omega_k|$.

If $\nu! = \nu_1! \cdots \nu_k!$, $|\nu| = \nu_1 + \cdots + \nu_k$, $\omega^\nu = \omega_1^{\nu_1} \cdots \omega_1^{\nu_k}$, $c_\nu = c_{\nu_1 \cdots \nu_k}$, $m_\nu = m_{\nu_1 \cdots \nu_k}$, then:

$$\Phi(\omega) = \sum\nolimits_{\nu_1+\cdots+\nu_k \le n} \frac{j^{|\nu|}}{\nu!} m_\nu \omega^\nu + o(|\omega|^n) \quad (22)$$

$$ln\Phi(\omega) = \sum\nolimits_{\nu_1+\cdots+\nu_k \le n} \frac{j^{|\nu|}}{\nu!} c_\nu \omega^\nu + o(|\omega|^n) \quad (23)$$

So, if $\nu_1 = \cdots = \nu_k = 1$, the k-th order moment and cumulant can be expressed as:

$$m_k = mom(x_1, \cdots, x_k) \quad (24)$$

$$c_k = cum(x_1, \cdots, x_k) \quad (25)$$

III. ENGINE BENCH TEST

The engine fault test was performed on a 6-cylinder in-line diesel engine. The test bench includes the following: a 6-cylinder in-line diesel engine, an AVL electric power dynamometer, a LMS Scada ||| noise and vibration test system and a computer. The power dynamometer was connected to the flywheel of the diesel engine through the coupling. The power dynamometer was used to control the engine during the test to maintain a constant load and relatively stable speed. Basic information about the engine is listed in Table 1.

TABLE 1. The main parameters of testing engine.

Items	Parameters
Type	Inline Diesel
Bore × Stroke	108 × 136 mm
Number of Cylinders	6
Intake Method	Turbocharged Inter-Cooled
Maximum Power	199 kW
Maximum Torque	1100N× m/1200-1600 rpm
Rated Speed	2300rpm

TABLE 2. The parameters of the engine testing equipment.

The Testing Equipment	Model	Remarks
Testlab Acoustic Vibration Testing and Analysis System	SCM05	LMS
Vibration sensor	621B40	PCB

The testing equipment used in experiment is shown in Table 2:

There are four vibration measuring points in this testing, and four acceleration sensors were installed on the cylinder head cover and block close to the first and third cylinder, respectively. The measuring range of acceleration sensors are 500 m/s^2, and the sensitivity are 50 mV/(m/s^2) and the resolution of are 0.02m/s^2. The sensor positions are shown in Fig 4.

In the process of testing, the sampling frequency will have important effect on the test results. Too low sampling frequency will cause the collected signal unable to contain fault features, leading to the failure of fault diagnosis. Too high sampling frequency will cause too large amount of data and too long time for signal analysis, which is not conducive to the realization of real-time fault diagnosis.

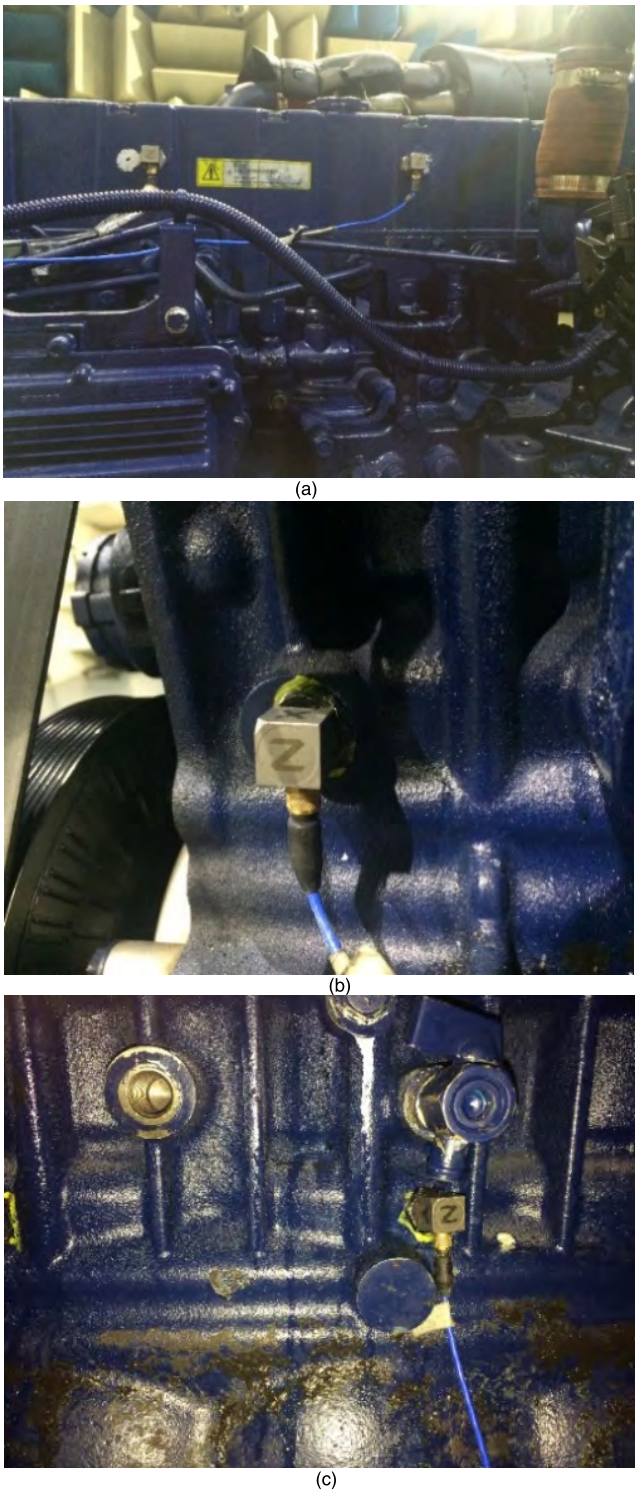

(a) (b) (c)

FIGURE 4. The measuring points. (a) Two measuring points on cylinder head cover. (b) The first measuring point on the block. (c) The second measuring point on the block.

Previous studies showed that the energy of diesel engine vibration signal is mainly concentrated in 10 kHz. According to the Nyquist's sampling theorem (the sampling frequency needs to be 2 times higher than the analytical frequency) and the previous pre-experiments, the sampling frequency was 25600 Hz, and the analysis frequency was 12800 Hz. Because of the excellent ability for identifying the fault characteristics, the Y-direction (the horizontal which is perpendicular to crankshaft) signal is chosen to analyze the vibration.

IV. THE OPTIMIZATION OF VMD

A. THE ANALYSIS OF VMD

VMD algorithm has a shortcoming that the number of modes, K, has to be set manually and properly. An inaccurate selection can cause over/under decomposition. Hence, to solve this problem, there are two most frequently used methods. The first one is determining a fixed K by priori knowledge. The second one is decomposing signals with VMD in several different K, and then selecting the best by comparison. The first method is convenient and efficient for analyzing simple vibration signals, but engine has so many unknown vibration sources that one fixed K cannot be suitable for every work condition. The second method can get the optimal value of every signal, but its calculation efficiency is too low. As there is not a generally accepted method for selecting K, a new idea is proposed in this paper.

As shown above, the main process of VMD is an iteration of u_k and ω_k. Relatively, the center frequencies ω_k is easier to control. Dragomiretskiy et al provided three ways to initialize ω_k in original VMD [17]: initializing ω_k to zero, initializing ω_k linearly and initializing ω_k randomly. Thereinto, initializing ω_k randomly leads to the highly random results, and initializing ω_k to zero is suitable for the signals with narrow bandwidth in low frequencies, while initializing ω_k linearly is suitable for the signals with wide bandwidth, which have the same characteristic as engine vibration signals.

Besides accuracy, ω_k also has a significant effect on the number of iterations which reflects calculation efficiency. In other words, if the initial values of ω_k are set properly, the iteration will converge quickly. Therefore, the initial values of ω_k need to be set as the characteristic frequencies of engine faults in order to improve calculation efficiency under high accuracy without over/under decomposition. The initial values don not require high precision, but need taking into account several characteristics of different working conditions. Taking above experiments as an example, how to estimate initial values of ω_k and K is explained as follows.

B. THE OPTIMIZATION METHOD

As among all kinds of engine faults, the fuel injection failure and valve clearance failure are common and difficult to distinguish, 50 sets of signals of fuel injection failure, big valve clearance failure, small valve clearance failure and normal working condition in the conditions are selected. The engine working condition is at 2100 rpm and 100% load. At this speed, each working cycle takes 0.057 s. The length of each set of signal for analysis is 0.06 s, and this length ensures each set of the analysis signals to contain a complete working cycle.

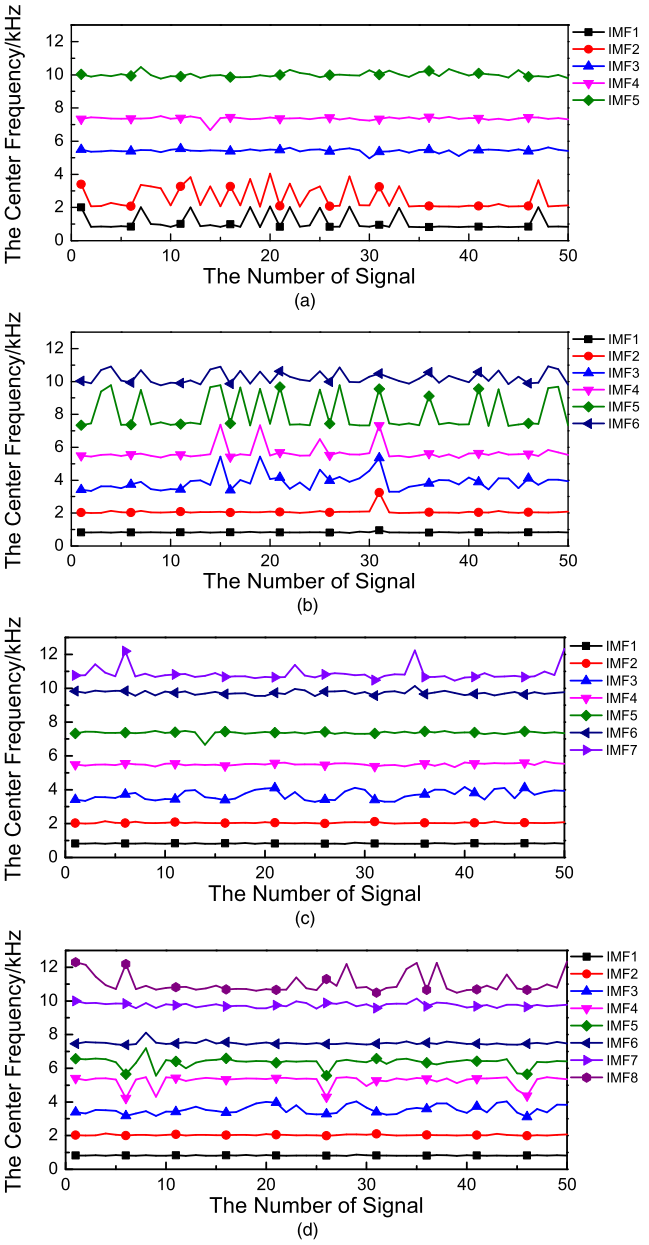

FIGURE 5. The decomposition results of fuel injection failure. (a) K = 5. (b) K = 6. (c) K = 7. (d) K = 8.

When the outtake valve clearance of first cylinder increases by 0.1 mm and the intake valve clearance of third cylinder increases by 0.1 mm in big valve clearance condition, the outtake valve clearance of first cylinder reduces by 0.1 mm and the intake valve clearance of third cylinder is reduces by 0.1 mm in small valve clearance condition.

To determine suitable ω_k initial values and K, all of the 200 sets of signals are decomposed in K = 5/6/7/8 and the center frequencies of each mode are shown as Fig 5-8:

To determine suitable K in all conditions, the figures need to be analyzed as follows. In fuel injection failure condition,

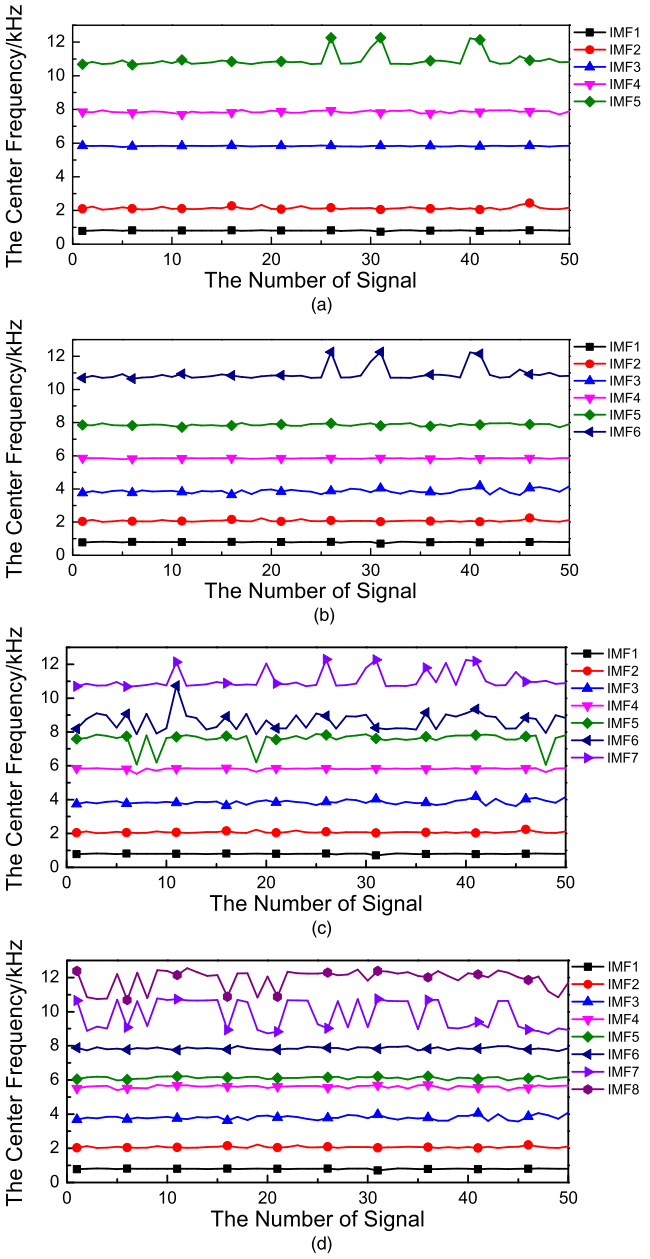

FIGURE 6. The decomposition results of big valve clearance. (a) K = 5. (b) K = 6. (c) K = 7. (d) K = 8.

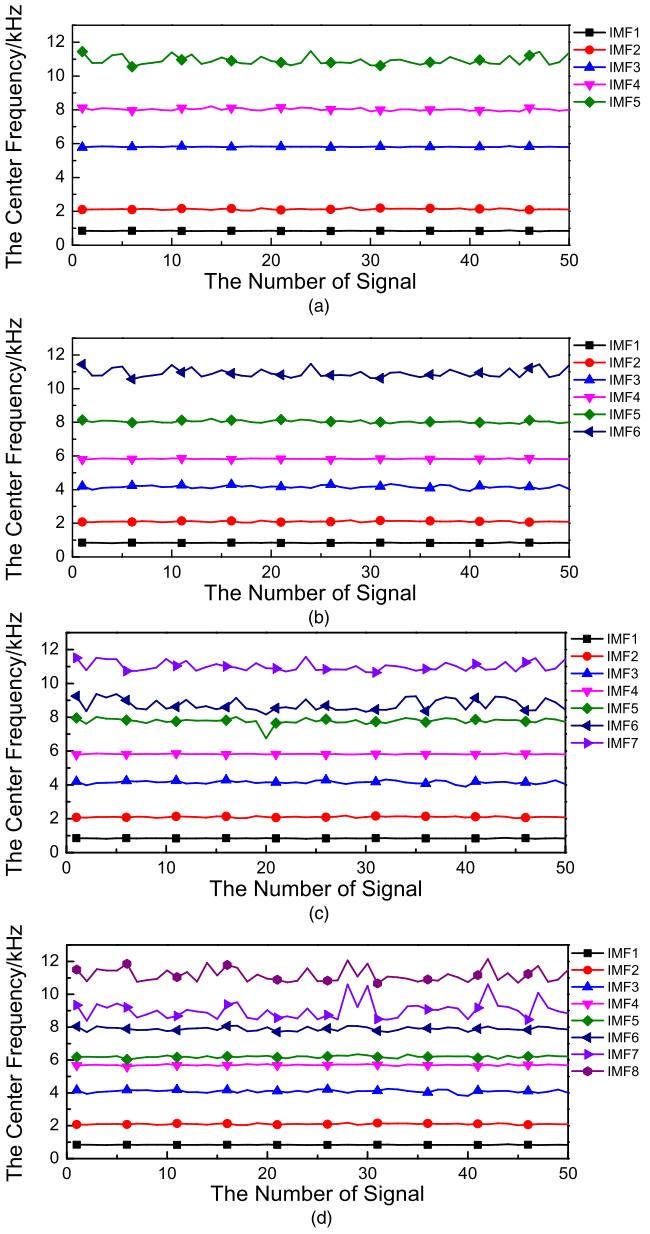

FIGURE 7. The decomposition results of small valve clearance. (a) K = 5. (b) K = 6. (c) K = 7. (d) K = 8.

K = 7 is the best value, because when K < 7, the center frequency curves fluctuate extremely due to the complexity of components in a mode, which is under decomposition. When K > 7, some center frequencies are quite close to each other, which is over decomposition. In the big valve clearance, small valve clearance and normal working condition, K = 6 is the best value, because when K < 6, the deviation between IMF2 and IMF3 is significant, which is also under decomposition. When K > 6, some center frequencies fluctuate extremely and are quite close to each other. According to above, the average values of center frequencies with the best value of K are computed and shown in Table 3.

Therefore, K is set as 6 and the initial values of center frequencies corresponding to K are: 0.82kHz, 2.11kHz, 3.93kHz, 5.75kHz, 7.70kHz, 10.49kHz. Thereinto, the first to fifth values are the average of all IMF, and the sixth value is the average of IMF6 and IMF7. Based on that, the center frequencies of the every 50 sets of signals are shown in Fig 9-12:

In summary, the core method of optimization for decomposition level in VMD is: selecting the best K for most signals by comparison and getting the center frequencies of engine vibration components. And then, those center frequencies can be taken as the initial values to control alternative processes in order to get IMF components in expected frequencies quickly. It also can reduce the effect of K selection on results.

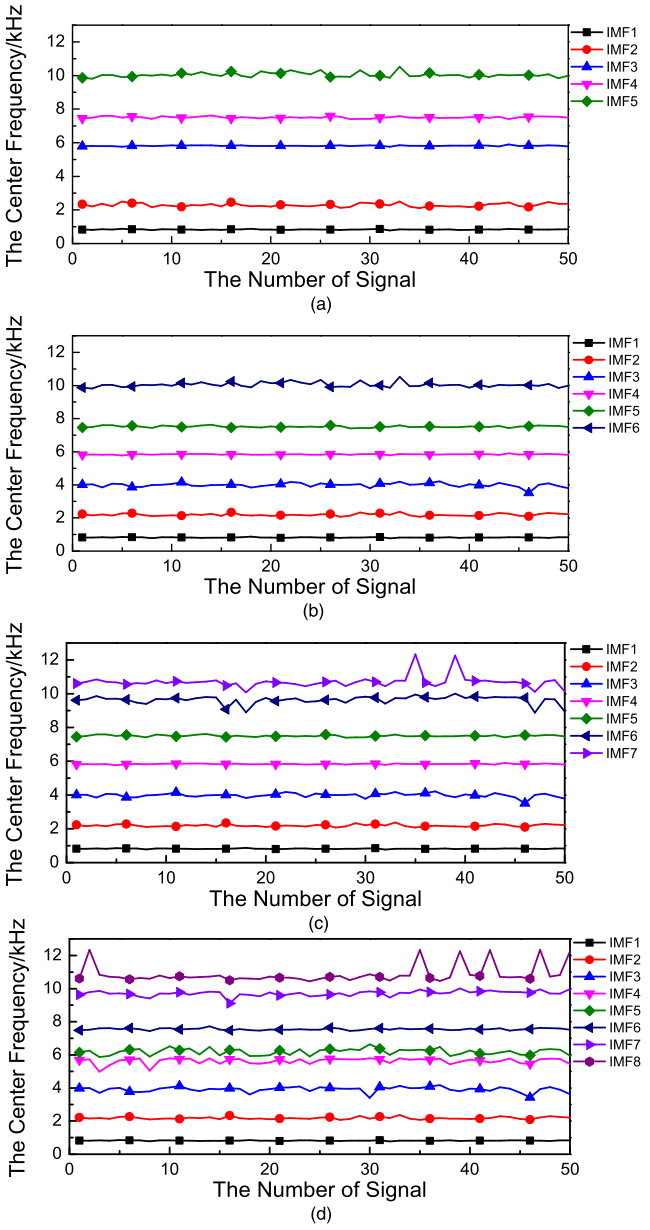

FIGURE 8. The decomposition results of normal working condition. (a) K = 5. (b) K = 6. (c) K = 7. (d) K = 8.

As shown in figures, the optimization achieves ideal results that adjacent IMFs have reasonable different values between each other and fluctuate gently. Besides, the average number of iterations reduced by 15%. Especially for fuel injection failure, there is not an over or under decomposition when K = 6.

In particular, the quadratic penalty term α is taken as the proven best value: 8400.

V. FAULT DIAGNOSIS

A. THE FAULT DIAGNOSIS METHOD

The VMD algorithm has a disadvantage that it cannot distinguish different signal sources with the same (or very similar) frequencies. ICA is introduced to solve the above-mentioned

TABLE 3. The average values of center frequencies.

The Average Values of Center Frequencies (kHz)	IMF 1	IMF 2	IMF 3	IMF 4	IMF 5	IMF 6	IMF 7
The Fuel Injection Condition	0.82	2.05	3.69	5.50	7.37	9.73	10.85
The Big Valve Clearance Condition	0.80	2.08	3.87	5.84	7.87	10.93	
The Small Valve Clearance Condition	0.84	2.10	4.16	5.83	8.04	10.92	
The Normal Working Condition	0.82	2.19	3.99	5.84	7.52	10.04	

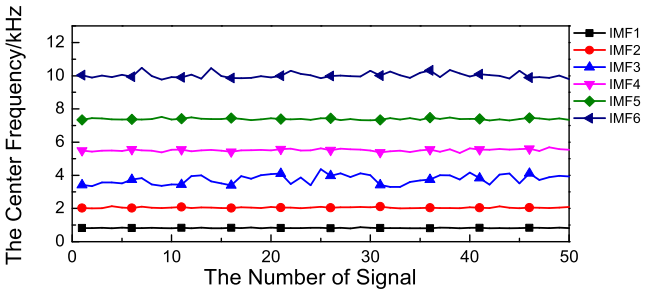

FIGURE 9. The fuel injection failure.

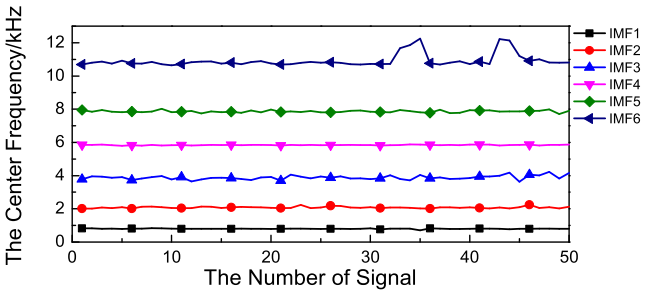

FIGURE 10. The big valve clearance.

trouble, but it cannot compose single channel signal, so ICA is combined into VMD for complementary advantages.

Through comparing the three ICA methods with each other in accuracy and calculation efficiency, Robust ICA is the best one, but it is not noteworthy enough to expound concretely in this extent limited paper. So, unless otherwise mentioned, all through this text the ICA means Robust ICA.

Original signal is decomposed by VMD firstly, and then the fourth-order cumulant of restructure signal turns into the first fault index (FI1). The results of VMD are decomposed by Robust ICA again, and then the fourth-order cumulant of this restructured signal turns into the second fault index (FI2).

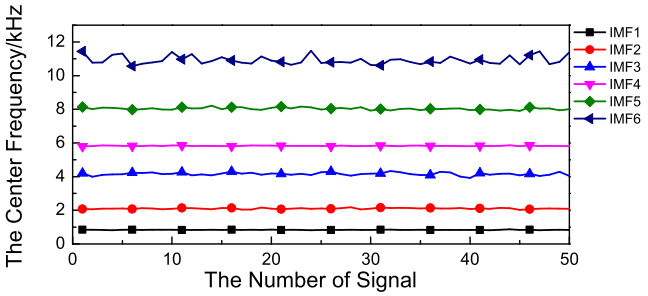

FIGURE 11. The small valve clearance.

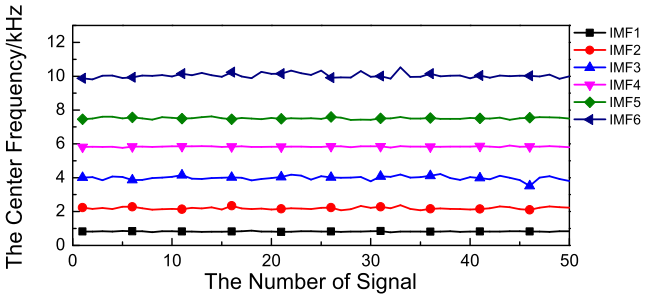

FIGURE 12. The normal working condition.

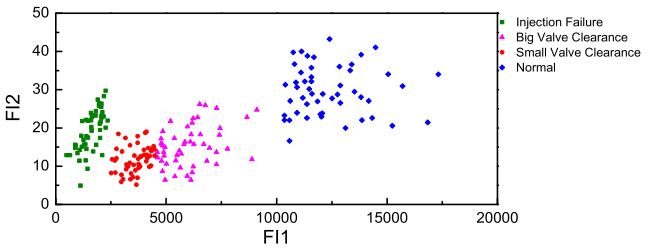

FIGURE 13. The scatter plot of different fault conditions.

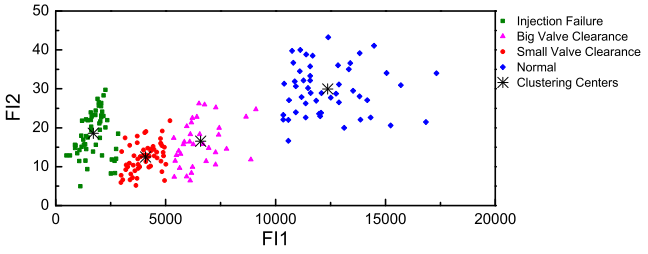

FIGURE 14. The results of original FCM.

Both FI1 and FI2 are taken as input parameters of FCM to detect faults.

Scatter plot of the 200 sets of signals in different fault conditions is shown in Fig 13:

The result of original FCM is shown in Fig 14:

The detailed explanations are shown in Table 4:

According to Table 4, the whole recognition rate is 89% (22 points are diagnosed wrongly in all of the 200 points). The results for the small sample is not satisfactory, which shows original FCM cannot be applied to engine fault detection directly. Based on the normal working condition with high accuracy, optimization is proposed. By means of analyzing

TABLE 4. The detailed explanations for the results.

The Working Condition	The Fuel Injection Failure	The Big Valve Clearance	The Small Valve Clearance	The Normal Working Condition
the Recognition Rate	88%	70%	62%	100%
the Explanations	7 sets of signals in small valve clearance are recognised as fuel injection failure	15 sets of signals are not recognised	7 sets of signals are not recognised and 15 sets of signals in big valve clearance are recognised as small valve clearance	the diagnosis is all correct

one of the fault conditions and the normal condition by FCM, two cluster centers were obtained (FCM require at least two clusters). After that, through analyzing every fault condition respectively, each fault condition cluster center and three normal working condition cluster centers were obtained. The average of three normal working condition cluster centers is taken as the final value (the result shows that the three values are very close to each other). Finally, the Euclidean distance between a certain scatter point and one of the cluster center is taken as the parameter to distinguish different faults. The flow chart of diagnosis is shown as Fig 15.

The cluster centers obtained by above method are shown in the Table 5:

To determine a suitable cluster center, the Euclidean distance between every point and corresponding cluster center is shown as Fig 16-19:

As shown in Fig 16, in the situation that taking the cluster center of fuel injection failure as reference point, the discrimination among different working conditions is obvious and the coincidence degree of every working point is extremely low. As shown in Fig 17, in the situation that taking the cluster center of big valve clearance as reference point, the coincidence degree between fuel injection failure and normal working condition is very high, which means those two working conditions can't be distinguished. As shown in Fig 18, in the situation that taking the cluster center of small valve clearance as reference point, the coincidence degree between fuel injection failure and big valve clearance is too high. As shown in Fig 19, in the situation that taking the cluster center of normal working condition as reference point, the discrimination among different working conditions is obvious, but some working points in big valve clearance and normal working conditions are too close to each other. Meanwhile, compared with the maximum values, the minimum values of normal working condition in different situations are very stable.

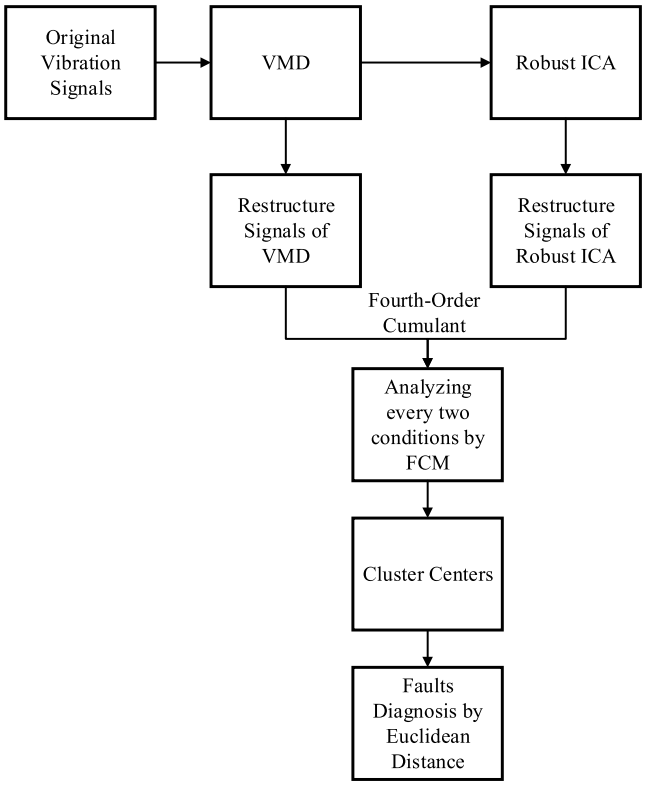

FIGURE 15. The flow chart of diagnosis.

TABLE 5. The cluster centers.

the Working Condition	the Fuel Injection Failure	the Big Valve Clearance	the Small Valve Clearance	the Normal Working Condition
the Cluster Centers	1609	5946	3623	12346
	19	15	12	30

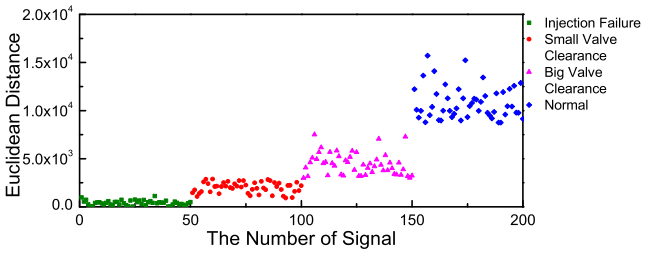

FIGURE 16. The Euclidean distance to the cluster center of fuel injection failure.

So, taking normal working condition at the maximum region is reasonable. In summary, as shown in Fig 16-19, taking cluster center of fuel injection failure as reference point achieved the highest accuracy. Based on that, the threshold is obtained:

If the Euclidean distance to cluster center of fuel injection failure: $\leq$ 1000, the condition is recognized as fuel injection failure.

If the Euclidean distance to the cluster center of fuel injection failure: 1000-2900, the condition is recognized as small valve clearance.

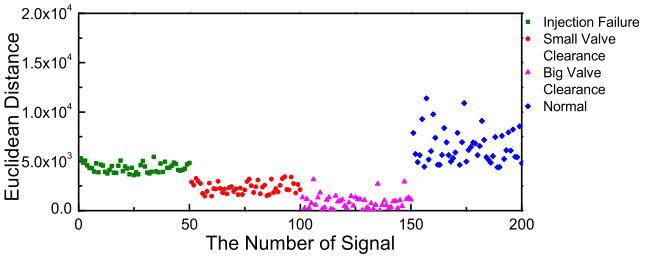

FIGURE 17. The Euclidean distance to the cluster center of big valve clearance.

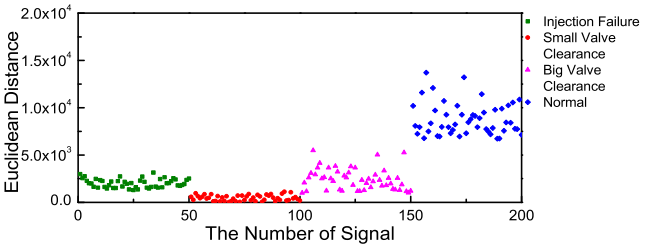

FIGURE 18. The Euclidean distance to the cluster center of small valve clearance.

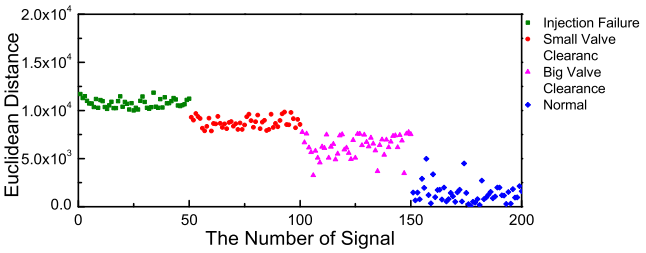

FIGURE 19. The Euclidean distance to the cluster center of normal working condition.

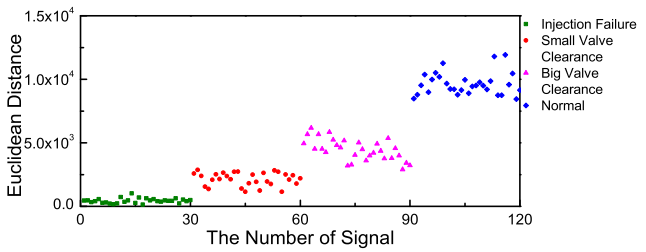

FIGURE 20. The diagnosis result of measured signals.

If the Euclidean distance to the cluster center of fuel injection failure: 2900-7500, the condition is recognized as big valve clearance.

If the Euclidean distance to the cluster center of fuel injection failure: $>$ 8500, the condition is recognized as normal working condition.

B. VERIFICATION

1) THE VERIFICATION OF MEASURED SIGNALS

In order to verify the accuracy of threshold proposed in this paper, authors selected another 30 sets of signals of fuel injection failure, big valve clearance failure, small valve clearance failure and normal working condition to distinguish by the method above. The result is shown as Fig 20. There are

only 1 set of fuel injection failure signal and 2 sets of big valve clearance signal recognized erroneously and the recognition rare is 98.3%. The result proved that the method proposed in this paper can diagnose different working conditions. Compared with original FCM, the above method has a prominent improvement, which is expected to be applied in engineering practice.

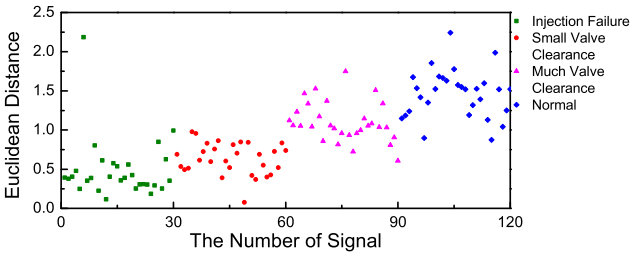

FIGURE 21. The diagnosis result of kurtosis index.

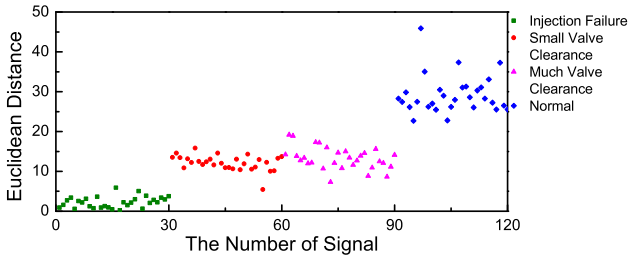

FIGURE 22. The diagnosis result of variance index.

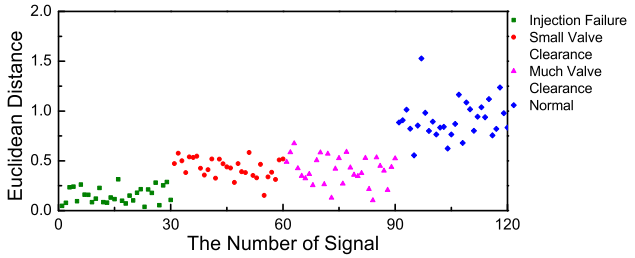

FIGURE 23. The diagnosis result of square root amplitude index.

2) THE VERIFICATION FOR ADVANTAGE OF THE FOURTH-ORDER CUMULANT

Kurtosis, skewness, variance, square root amplitude, entropy, the maximum singular value, the fourth-order cumulant and so on are all high frequently used indexes in faults diagnosis. Among those, when the fourth-order cumulant of Gaussian stochastic signal is 0, it can reduce the effect of Gaussian noise. Besides, the fourth-order cumulant has good ability in recognizing nonlinear components and can magnify the difference between different working condition signals. The fourth-order cumulant is selected as feature parameter to diagnose engine faults. In order to prove the advantage of the fourth-order cumulant, authors selected kurtosis, variance and square root amplitude as feature parameters to diagnose above 120 sets of signals with the method proposed in this paper. In particular, authors also researched the other indexes and only the best three ones are selected to be shown in Fig 21, Fig 22 and Fig 23.

As shown in Fig 21, the effect of kurtosis index is negative. The threshold of different working conditions is fuzzy. As shown in Fig 22, the variance index can't distinguish the small valve clearance and big valve clearance accurately. As shown in Fig 23, besides small valve clearance and big valve clearance, the square root amplitude index can't distinguish fuel injection failure either. Compared with those indexes, the fourth-order cumulant shown in Fig 20 has the highest accuracy. The results prove that the fourth-order cumulant has advantage in faults diagnosis.

3) THE COMPARISON WITH LEAST SQUARES SUPPORT VECTOR MACHINE

The Least Squares Support Vector Machine (LSSVM) is a classic classifier. The fourth-order cumulant of VMD decomposition reconstruction signal (FI1) and Robust ICA reconstruction signal (FI2) was used as the fault diagnosis features. The LSSVM classifier is trained with respectively 20 sets of fuel injection failure, small valve clearance, big valve clearance and normal working condition. And 30 sets of signals mentioned above are taken as test samples, the analysis is carried out by using LSSVM classifier. In LSSVM analysis, RBF_kernel is used as kernel function. When regularization parameter is 0.1, kernel parameter is 0.1 and multilevel classification coding is code_MOC (Minimum output coding). The analysis result is shown in Fig 24.

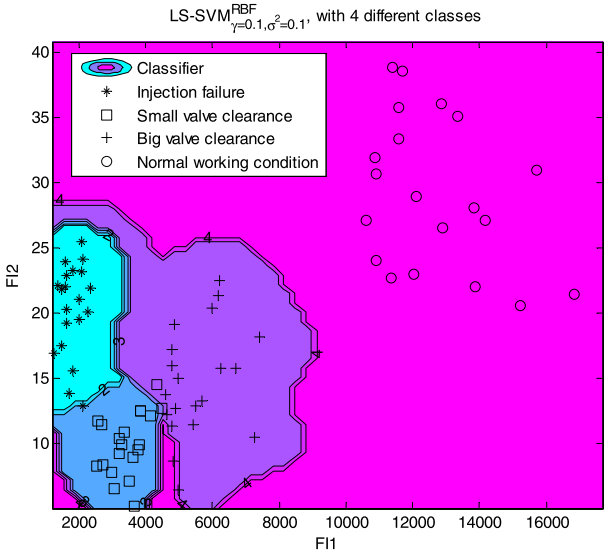

FIGURE 24. The diagnosis result of LSSVM.

As shown in Fig 24, the four different working conditions can be broadly distinguished from each other. However, there are still many samples that cannot be correctly distinguished, especially small and big valve clearance. The recognition rate is 79.17%, which is much lower than FCM method. The LSSVM method used in this paper is not fully optimized, and the recognition rate of LSSVM will rise after optimization. However, optimization will increase complexity of diagnosis process. So, the method proposed in this paper is better.

In summary, the optimized method proposed in this paper has a prominent improvement, which is expected to be applied in engineering practice.

VI. CONCLUSION AND OUTLOOK

In order to realize the detection of various different faults by single channel vibration signal, several algorithms are optimized. The main conclusions are as follows:

1) To solve the problem that the number of modes in VMD is selected manually, 200 sets of signals in different working conditions are analyzed. Based on characteristics of VMD and signals, the initial values of center frequencies are optimized and the optimization improves calculation efficiency under high accuracy.
2) VMD can't decompose signals with the same frequency, so Robust ICA is introduced in this paper for complementary advantages. The fourth-order cumulant of extraction from VMD and Robust ICA decomposition is taken as faults indices.
3) To improve the accuracy of faults diagnosis, the Euclidean distance to cluster center of fuel injection failure is taken as a parameter to distinguish different faults, which get a satisfactory result. Through comparison, the method proposed in this paper is proved to have certain advantages.

There are also many problems to be solved, such as:

1) More fault types need to be analyzed.
2) The calculation efficiency should be improved further.
3) Authors also will continue carrying out experiments and calculations on faults diagnosis of a series of working conditions (including unsteady working conditions) to build database of faults diagnosis and researching on the universal diagnosis method.

REFERENCES

[1] Z. Gao, C. Cecati, and S. X. Ding, "A survey of fault diagnosis and fault-tolerant techniques—Part I: Fault diagnosis with model-based and signal-based approaches," *IEEE Trans. Ind. Electron.*, vol. 62, no. 6, pp. 3757–3767, Jun. 2015.

[2] F. Elamin, Y. Fan, F. Gu, and A. Ball, "Diesel engine valve clearance detection using acoustic emission," *Adv. Mech. Eng.*, vol. 2010, no. 2, pp. 1652–1660, 2010.

[3] Y. Pan, J. Chen, and X. Li, "Bearing performance degradation assessment based on lifting wavelet packet decomposition and fuzzy C-means," *Mech. Syst. Signal Process.*, vol. 24, no. 2, pp. 559–566, 2010.

[4] N. Tandon and A. Choudhury, "A review of vibration and acoustic measurement methods for the detection of defects in rolling element bearings," *Tribol. Int.*, vol. 32, no. 8, pp. 469–480, Aug. 1999.

[5] C. Sheng, T. Wu, and Y. Zhang, "Non-destructive testing of marine diesel engines using integration of ferrographic analysis and spectrum analysis," *Insight-Non-Destructive Test. Condition Monit.*, vol. 54, no. 7, pp. 394–398, 2012.

[6] X. P. Yan, C. H. Zhao, Z. Y. Lu, X. C. Zhou, and H. L. Xiao, "A study of information technology used in oil monitoring," *Tribol. Int.*, vol. 38, no. 10, pp. 879–886, 2005.

[7] J. Zhang *et al.*, "Diesel engine noise source identification based on EEMD, coherent power spectrum analysis and improved AHP," *Meas. Sci. Technol.*, vol. 26, no. 9, 2015, Art. no. 095010.

[8] S. F. Taglialatela, N. Cesario, M. Lavorgna, and B. M. Vaglieco, "Diagnosis and control of advanced diesel combustions using engine vibration signal," in *Proc. SAE World Congr. Exhib.*, Detroit, MI, USA, 2011, Paper 2011-01-1414.

[9] M. Zadnik, F. Vincent, R. Vingerboeds, and F. Galtier, "SI engine knock detection method robust to resonance frequency changes," in *Proc. 8th Int. Conf. Engines Automobiles (ICE)*, Naples, Italy, vol. 15, 2007, Paper 2007-24-0054.

[10] Y. Wang, Y. Si, B. Huang, and Z. Lou, "Survey on the theoretical research and engineering applications of multivariate statistics process monitoring algorithms: 2008–2017," *Can. J. Chem. Eng.*, vol. 96, no. 10, pp. 2073–2085, 2018.

[11] D. Siano and D. D'Agostino, "Knock detection in si engines by using the discrete wavelet transform of the engine block vibrational signals," *Energy Procedia*, vol. 81, pp. 673–688, Dec. 2015.

[12] X. Wang, C. Liu, F. Bi, X. Bi, and K. Shao, "Fault diagnosis of diesel engine based on adaptive wavelet packets and eemd-fractal dimension," *Mech. Syst. Signal Process.*, vol. 41, nos. 1–2, pp. 581–597, 2013.

[13] A. Bustos, H. Rubio, C. Castejón, and J. C. García-Prada, "EMD-based methodology for the identification of a high-speed train running in a gear operating state," *Sensors*, vol. 18, no. 3, p. 793, 2018.

[14] N. E. Huang *et al.*, "The empirical mode decomposition and the Hilbert spectrum for nonlinear and non-stationary time series analysis," *Proc. Roy. Soc. London Ser. A, Math., Phys. Eng. Sci.*, vol. 454, no. 1971, pp. 903–995, Mar. 1998.

[15] B. Chen, Z. He, X. Chen, H. Cao, G. Cai, and Y. Zi, "A demodulating approach based on local mean decomposition and its applications in mechanical fault diagnosis," *Meas. Sci. Technol.*, vol. 22, no. 5, 2011, Art. no. 055704.

[16] Z. Wu and N. E. Huang, "Ensemble empirical mode decomposition: A noise-assisted data analysis method," *Adv. Adapt. Data Anal.*, vol. 1, no. 1, pp. 1–41, 2008.

[17] K. Dragomiretskiy and D. Zosso, "Variational mode decomposition," *IEEE Trans. Signal Process.*, vol. 62, no. 3, pp. 531–544, Feb. 2014.

[18] K. Dragomiretskiy and D. Zosso, "Two-dimensional variational mode decomposition," in *Proc. 10th Int. Workshop Energy Minimization Methods Comput. Vis. Pattern Recognit.*, Hong Kong, vol. 8932. Berlin, Germany: Springer-Verlag, 2015, pp. 197–208.

[19] C. Yi, Y. Lv, and Z. Dang, "A fault diagnosis scheme for rolling bearing based on particle swarm optimization in variational mode decomposition," *Shock Vib.*, vol. 2016, no. 2, 2016, Art. no. 9372691.

[20] Z. Lv, B. Tang, Y. Zhou, and C. Zhou, "A novel method for mechanical fault diagnosis based on variational mode decomposition and multikernel support vector machine," *Shock Vib.*, vol. 2016, no. 5, 2016, Art. no. 3196465.

[21] N. Huang, H. Chen, G. Cai, L. Fang, and Y. Wang, "Mechanical fault diagnosis of high voltage circuit breakers based on variational mode decomposition and multi-layer classifier," *Sensors*, vol. 16, no. 11, p. 1887, 2016.

[22] X. Zhang, D. Jiang, T. Han, N. Wang, W. Yang, and Y. Yang, "Rotating machinery fault diagnosis for imbalanced data based on fast clustering algorithm and support vector machine," *J. Sensors*, vol. 2017, no. 12, 2017, Art. no. 8092691.

[23] Z. Wang, L. Jia, and Y. Qin, "Adaptive diagnosis for rotating machineries using information geometrical kernel-ELM based on VMD-SVD," *Entropy*, vol. 20, no. 1, pp. 73–90, 2018.

[24] D. Han, X. Su, and P. Shi, "Weak fault signal detection of rotating machinery based on multistable stochastic resonance and VMD-AMD," *Shock Vib.*, vol. 2018, no. 4, 2018, Art. no. 4252438.

[25] Z. Lou, D. Shen, and Y. Wang, "Two-step principal component analysis for dynamic processes monitoring," *Can. J. Chem. Eng.*, vol. 96, no. 1, pp. 160–170, 2018.

[26] T.-W. Lee, "Independent component analysis," in *Independent Component Analysis*. Boston, MA, USA: Springer, 1998, pp. 27–66.

[27] A. Hyvarinen, "A family of fixed-point algorithms for independent component analysis," in *Proc. IEEE Int. Conf. Acoust., Speech, Signal Process.*, Apr. 1997, pp. 3917–3920.

[28] N. B. Jones and Y.-H. Li, "A review of condition monitoring and fault diagnosis for diesel engines," *Lubrication Sci.*, vol. 6, no. 3, pp. 267–291, 2000.

[29] A. J. C. Sharkey, G. O. Chandroth, and N. E. Sharkey, "A multi-net system for the fault diagnosis of a diesel engine," *Neural Comput. Appl.*, vol. 9, no. 2, pp. 152–160, 2000.

[30] M. Tamura, H. Saito, Y. Murata, K. Kokubu, and S. Morimoto, "Misfire detection on internal combustion engines using exhaust gas temperature with low sampling rate," *Appl. Thermal Eng.*, vol. 31, nos. 17–18, pp. 4125–4131, 2011.

[31] Y. E. Shao, C.-J. Lu, and Y.-C. Wang, "A hybrid ICA-SVM approach for determining the quality variables at fault in a multivariate process," *Math. Problems Eng.*, vol. 2012, Jul. 2012, Art. no. 284910.
[32] Z. Uddin, A. Ahmad, M. Iqbal, and Z. Kaleem, "Adaptive step size gradient ascent ICA algorithm for wireless MIMO systems," *Mobile Inf. Syst.*, vol. 2018, no. 1, 2018, Art. no. 7038531.
[33] Y.-B. Jing, C.-W. Liu, F.-R. Bi, X.-Y. Bi, X. Wang, and K. Shao, "Diesel engine valve clearance fault diagnosis based on features extraction techniques and FastICA-SVM," *Chin. J. Mech. Eng.*, vol. 30, no. 4, pp. 991–1007, 2017.
[34] J. C. Bezdek, "Pattern recognition with fuzzy objective function algorithms," *Adv. Appl. Pattern Recognit.*, vol. 22, no. 1171, pp. 203–239, 1981.
[35] Z. Xianda. *Time Series Analysis: Higher Order Statistics Method*. Beijing, China: Tsinghua Univ. Press, 1996.

XIAOYANG BI received the degree from Tianjin University, Tianjin, China, in 2012, where she is currently pursuing the Ph.D. degree in mechanics. Her current research interests include vibration control, fault diagnosis, and signal processing.

SHUQIAN CAO received the Ph.D. degree in general and fundamental mechanics from Tianjin University, Tianjin, China, in 2003, where he is currently a Professor and a Doctoral Advisor. His current research interests include nonlinear dynamics and control, structural dynamics and modal analysis, rotor dynamics, nonlinear dynamics of piezoelectric intelligent structure, fault diagnosis, and mechanism analysis.

DAMING ZHANG received the Ph.D. degree in engineering mechanics from Iowa State University, Ames, IA, USA, in 1997. He is currently a Professor with California State University, Fresno, CA, USA. His current research interests include engine technology and vehicle development, noise estimation and reduction, as well as finite element and boundary element analysis in automotive, aerospace, semiconductor, and optoelectronic industries.